




# Development of High-Pressure Transducer: Design, Finite Element and Experimental Analysis

S. Rab<sup>1\*</sup> , S. Yadav<sup>2</sup>, A. Haleem<sup>3</sup> and A. Zafer<sup>2</sup>

<sup>1</sup>School of Architecture, Technology, and Engineering, University of Brighton, Brighton, UK

<sup>2</sup>CSIR-National Physical Laboratory (CSIR-NPL), New Delhi, India

<sup>3</sup>Department of Mechanical Engineering, Jamia Millia Islamia, New Delhi, India

Received: 21 January 2023 / Accepted: 20 March 2023 / Published online: 30 March 2023

© Metrology Society of India 2023

**Abstract:** Over the past few decades, the rapid and expanding usage of high-pressure technologies in science and engineering has prompted researchers to focus on developing better instruments and technologies with improved measurement uncertainties for various applications. Such efforts resulted in the development of new and advanced measurement techniques and standards to address calibration challenges and provide traceability to users. In the present study, an indigenous strain gauge-type pressure transducer has been designed, developed, tested, and calibrated for pressure measurements up to 1000 MPa. The sensing element's cylindrical shape was used, providing a cost-effective and straightforward approach for designing a pressure transducer over a wide pressure range. It also ensures a leak-proof and locked connection to the external environment, with no over-constrained contacts. The calibration and performance checking of the pressure transducer has been carried out using the national primary pressure standard with the internationally accepted calibration procedure. The transducer response under pressure is highly linear during its performance evaluation. As a result, the transducer performs satisfactorily within the reasonable measurement uncertainty of 0.5% of the full scale. The pressure transducer developed may help trace the user industries and calibration laboratories in the high range of pressure measurement and serve as a pressure transfer standard.

**Keywords:** Pressure; Metrology; FEA; Accuracy; Transducer; Uncertainty

## 1. Introduction

The industrial application of pressure metrology has grown in importance during the last few decades. Pressure measuring devices use a variety of principles and approaches to measure pressure. In general, a mechanical device responds directly to changes in pressure, such as a change in the length of a mercury column or up and down movement of the piston in the piston-cylinder (P–C) assembly, or in other cases, a change in mechanical stresses or a change in the resistance of a coil. Thus, the response function of a pressure-induced change can thus be measured, and quantitative data can be obtained [1–5].

A wide variety of pressure transducers are available commercially. These pressure measuring devices capable of comparing/verifying/calibrating another pressure

measuring device's reading may be direct or indirect pressure indicating devices. These devices might also find application as pressure standards if they are traceable to pressure standards of better measurement uncertainties. Traditionally, the calibration ratio is kept as 4:1. A pressure calibrator's accuracy is usually four times more accurate than the device under calibration. Sometimes, a lesser ratio is also used according to the type of application, for example, in inter-laboratory comparisons or proficiency testing, etc. [6–10].

In order to measure pressure, pressure measuring devices employ a number of principles and approaches. A mechanical device typically responds directly to a change in pressure, for example, by changing the height of the mercury column, the up-and-down movement of the piston in the piston-cylinder (P–C) assembly, the mechanical properties, or sometimes the resistance of the coil, the capacitance, etc. As a result, it is possible to monitor the response function with pressure-induced change and obtain

\*Corresponding author, E-mail: shanayrab753@gmail.com

quantitative data [1, 4]. Out of several mentioned techniques, in the past, pressure transducers of the strain gauge type were frequently utilised as a pressure standard in high-pressure metrological and industrial applications. These transducers are simple to make and economical. One of the advantages of such transducers is that, with the help of suitable electrical circuitry, they can be built with highly sharp resistance changes, allowing for the detection of minimal changes in resistance as a function of applied pressure. In such type of transducer, the gauges are not directly exposed to the pressure transmitting media but are behind or integrated into the deflecting component to avoid an effect of the pressure transmitting media on the gauge properties [11–15]. The diaphragm-based pressure transducers usually consist of tube-shaped elements, and their analytical investigations are carried out using the theory of pressure vessels. Analytical investigations of stress–strain behaviour and deflections are computed based on the available theoretical modelling [16–18].

Further, with modern design techniques, numerous analytical and simulation methods are available for computational investigations of pressure transducers. Such analysis is essential for investigating design-related issues. The computational techniques help simulation and virtual analysis under assumptions that predict specified design and behaviour. One such technique is Finite Element Analysis (FEA), which is more often used in computational investigations of mechanical systems wherein the discretisation of mechanical structure is differentiated into a finite number of similar parts, assuming they are homogenous and isotropic. Suitable boundary conditions are applied to the structure, and investigations are made accordingly. Such investigations help test and validate the theoretical/analytical findings before the actual development of any mechanical component [19–25]. The comprehension for designing and developing the pressure transducer is shown in Fig. 1. Analytical and computational methodologies are used, followed by experimental observations for validation.

In the present study, an indigenous strain gauge pressure transducer has been designed, fabricated, and tested at pressures up to 1000 MPa. The pressure transducer is calibrated and checked for performance using a dead-weight national pressure standard and an internationally established calibration technique. In the following subsequent sections, the step-by-step approach for the design and development of the transducer is briefly described.

## 2. Material and Design

The critical aspect of the design is the material selection of the transducer. Material selection in the high-pressure area

is crucial because the sensing element material yield strength limits the intensity of the applied pressure. Thus, different materials can be used for the pressure sensing element. Case Aermet-100 is used as transducer material because of its high strength and other mechanical properties [11, 16]. Aermet alloy is martensitic alloy steel with extremely high strength. Table 1 summarises the material properties of the Aermet alloy.

In most cases, cylindrical transducers use an elastic element in the form of a hollow cylinder, which can be designed with various materials depending on the desired pressure range. The design has a blind end on one side and is tightly attached to the pressure line. Although elastic element deformations are proportional to applied internal pressure, they are generally influenced by the state of stresses exerted on the transducer. Analytical calculations can only approximate the effects of deformation vs. applied pressure [17, 21].

The ‘Lamé equations’ are commonly employed in the theoretical analysis of the thick cylinder within the elastic limit. The calculations assume that tubes have both open ends, which is not the case in our scenario, as there is only one open end; however, this equation will hold when the tubes are not near the ends. In this investigation, the thick-walled cylinder is considered to withstand constant internal pressure. To address the problem, consider axisymmetry around the  $z$ -axis and solve the differential equations of stress equilibrium in polar coordinates. The radial and hoop stresses are denoted by the letters  $\sigma_r$  and  $\sigma_\theta$ , respectively. We can get the following results by combining the Lamé equations with the boundary conditions at any radius ( $r$ ) and internal pressure ( $P_i$ ).

$$\sigma_r = \frac{a^2 \cdot P_i}{b^2 - a^2} \left[ 1 - \left( \frac{b^2}{r^2} \right) \right] \quad (1)$$

$$\sigma_\theta = \frac{a^2 \cdot P_i}{b^2 - a^2} \left[ 1 + \left( \frac{b^2}{r^2} \right) \right] \quad (2)$$

where  $a$  and  $b$  consider as an internal radius and external radius, respectively. From the ‘Lamé criterion, Eq. 3 demonstrates the link between maximal von mises stress ( $P_{\max}$ ), yield strength ( $\sigma_y$ ), and transducer thickness ( $t = b - a$ ).

$$\frac{P_{\max}}{\sigma_y} = \frac{1}{\sqrt{3}} \left( \frac{b^2 - a^2}{b^2} \right) \quad (3)$$

The equation shows that two factors define the pressure transducer’s pressure-bearing capabilities. First, when the material’s yield strength is increased, the material’s pressure-bearing capacity is observed to increase. Second, a single material’s pressure-bearing capability rises with thickness, but only up to a particular thickness, called the “saturation thickness.” After this saturation thickness, the

**Fig. 1** Generalised flow chart for design and development of the pressure transducer

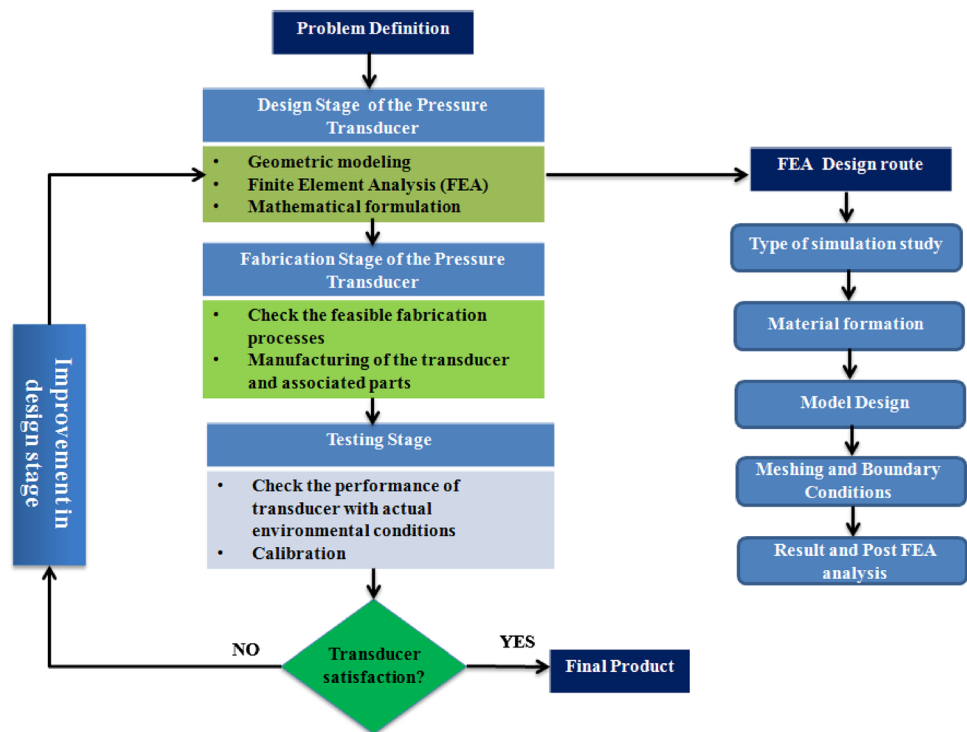


**Table 1** Physical Properties of Aermet-100

| Properties            | Value                       |
|-----------------------|-----------------------------|
| Density               | 7890 (kg/m <sup>3</sup> )   |
| Modulus of Elasticity | 195 × 10 <sup>9</sup> (Pa)  |
| Poisson's Ratio       | 0.3                         |
| Yield Strength        | 1.80 × 10 <sup>9</sup> (Pa) |

different thickness increases the cost and lowers the transducer's extreme sensitivity. Figure 2 shows the relationship between the thickness of the transducer with maximum allowable stress.

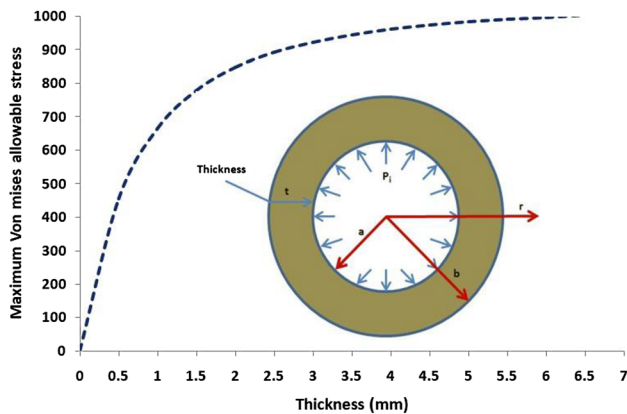


**Fig. 2** Maximum von mises allowable stress with a thickness

In high-pressure measuring instruments, leakage prevention design is essential. Thus to tackle the problem, a connection assembly is used to connect the pressure transducer to the high-pressurised fluid line to create a leak-proof design [14, 26, 27]. This design uses a high-strength cone (stainless steel) between the connector and transducer assembly. The conical surface of the cone provides perfect metal-to-metal contact between the connector and transducer for leakage prevention. Figure 3 shows a 3D model of the cone.

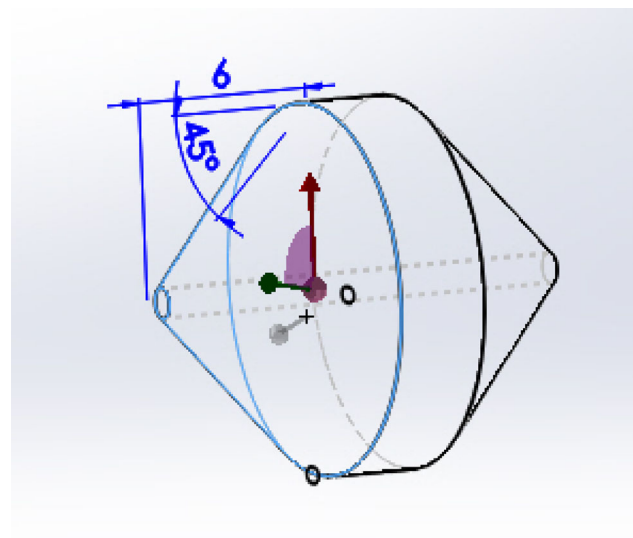


**Fig. 3** 3D model of the Cone

With the help of a 3D modelling tool (SolidWorks), a diaphragm-based transducer is designed after accounting for all leakage-related preventions. Figure 4 depicts a detailed drawing of the pressure transducer. During the design process, the proper shape is chosen, and the appropriate dimensions are calculated using mathematical model equations so that the transducer performs adequately or without failure up to the maximum desired pressure.

After modelling the sensing element, an outer cell is modelled with the help of a CAD modelling tool. It is applied to shield the sensing element from damage from the outside environment. The sensors and cables are likewise protected by this protective cell. A leaked route may form if the transducer material contains nonlinearity, allowing the transducer media to escape. These cells are required to prevent any accidents due to the high-pressure media. Figure 5 shows the 3D and fabricated model of the outer cell.

### 3. Computational Studies

Finite Element Analysis (FEA) is also used to investigate the behaviour of a transducer when it is subjected to high pressure. In the current context, the precision of the modelling of sensing elements, the applied boundary conditions, meshing into optimum-sized elements, material qualities, and loading conditions all have a role in the dependability and accuracy of FEA results. As a result, precise simulations aid in the development of better designs [28, 29].

As previously stated, the pressure detecting element is Aermet alloy steel. Table 1 shows the mechanical parameters of the chosen material. This type of high-strength steel has a chemical composition of C = 0.23%, Co = 13.40%, Ni = 11.10%, Cr = 3.10%, Mo = 1.20, and Ti = 0.05. Stress analysis was carried out under the maximum desired pressure to check any failure mechanism. Ansys

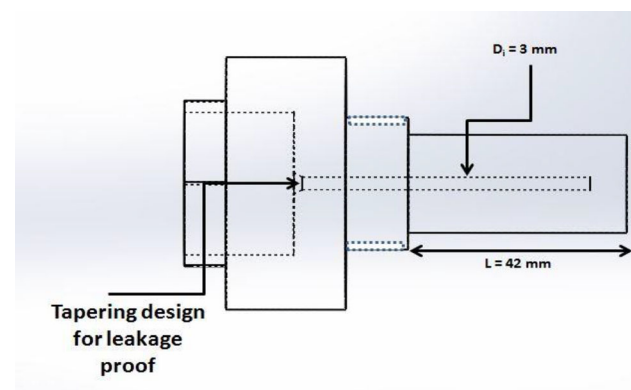


**Fig. 4** 2D drawing of the pressure transducer

Workbench, a simulation tool, is utilised to conduct stress analysis. This geometry generates a triangular mesh of sufficient size with a minimum Edge Length of 3.14160 mm. The total element and node numbers are, respectively, 3170 and 5361. Figure 6 depicts all of the applied boundary conditions with meshing.

Figure 7 summarises stress pattern under the maximum pressure condition. The stress is found to be within allowed limits at the maximum applied pressure (i.e. 1 GPa), with more than 1.5 factors of safety. The maximum hoop, radial, and axial stress are found at 1071.3 MPa,  $-1041 \text{ MPa}$  and  $-387 \text{ MPa}$ , respectively. The negative sign indicates the compressive nature of the generated stress in the pressure transducer.

## 4. Fabrication and Experimental Analysis

### 4.1. Fabrication of Pressure Transducer

Aermet alloy series steel-based pressure transducer is fabricated with the help of CNC and Lathe machines based on the dimensions of the pressure transducer. The fabrication process includes several processes, i.e. machining, turning, shaping, drilling, grinding, surfacing, etc. [30, 31]. Figure 8a shows one of the fabrication processes, and Fig. 8b shows the fabricated transducer with a cone.

### 4.2. Rigidity Test

To verify the investigated results of FEA, testing has been carried out using state-of-the-art and globally compatible national primary pressure standards for checking the rigidity of the pressure transducer under the maximum applied pressure. The standard used for testing the pressure transducers is a Controlled Clearance Type Piston Gauge (CCPG) primary pressure standard, designated as NPL-H1, capable of measuring pressure from (20–1000) MPa. The compatibility of the standard has been established through participation in international critical comparison exercises [32–34]. The maximum hydraulic pressure was applied to the transducer. As per the mathematical calculations, it also worked well in the experiment with the appropriate factor of safety.

### 4.3. Strain Gauging and Analysis

The pressure transducer undergoes finishing procedures in preparation for the attachment of strain gauges. The surface roughness of the flat surface at strain gauge locations is up to  $5 \mu\text{m}$ , which is acceptable for strain gauge use. For bonding, four foil-type strain gauges (size 5 mm, resistance 350, and gain factor 2.1) made by M/s Hytech Micro-

**Fig. 5** Outer cell of the transducer, **a** 3D CAD model and **b** Fabricated model

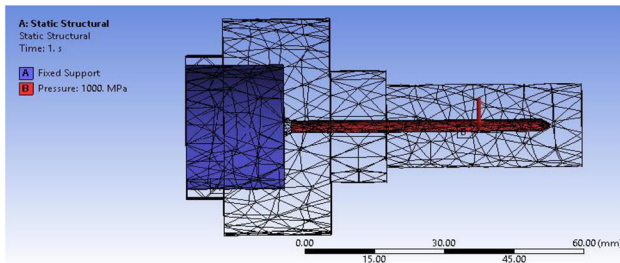
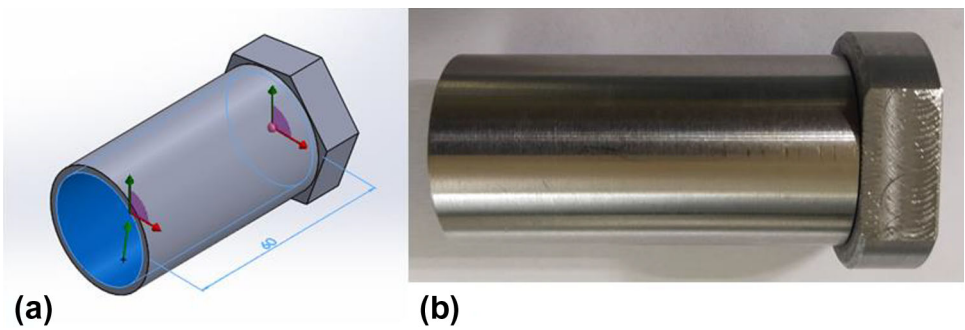


**Fig. 6** Meshing and boundary conditions on the pressure transducer

Measurements (P) Ltd, model AP2-3-5SD-C6-EL were purchased locally. According to the earlier finite element analysis of the selected geometry, the strain gauges were applied to the pressure transducer in a typical four-arm bridge arrangement [35, 36]. Thus, to make a Wheatstone bridge, two strain gauges were bonded on each hoop side

(over the outer surface of the transducer) and functioned as active gauges and two on the end side acted as dummy gauges. Figure 9a and b shows strain gauges arrangement and typical four bridge arrangement of gauges on the transducer.

The Wheatstone is made up of four strain gauges that are joined together. Different strain gauge arrangements provide different results in the configuration of a bridge. As a result, the transducer’s sensitivity varies.  $R_1$ ,  $R_2$ ,  $R_3$ , and  $R_4$  are the resistances of the strain gauges forming four arms of the full Wheatstone bridge, with  $R_1$  &  $R_3$  as active gauges and  $R_2$  &  $R_4$  as dummy gauges in the front face of the transducer (Minimum strains), then Kirchhoff’s law is used to calculate the output voltage ( $V_o$ ) concerning the excitation voltage ( $V_{ex}$ ), as follows;

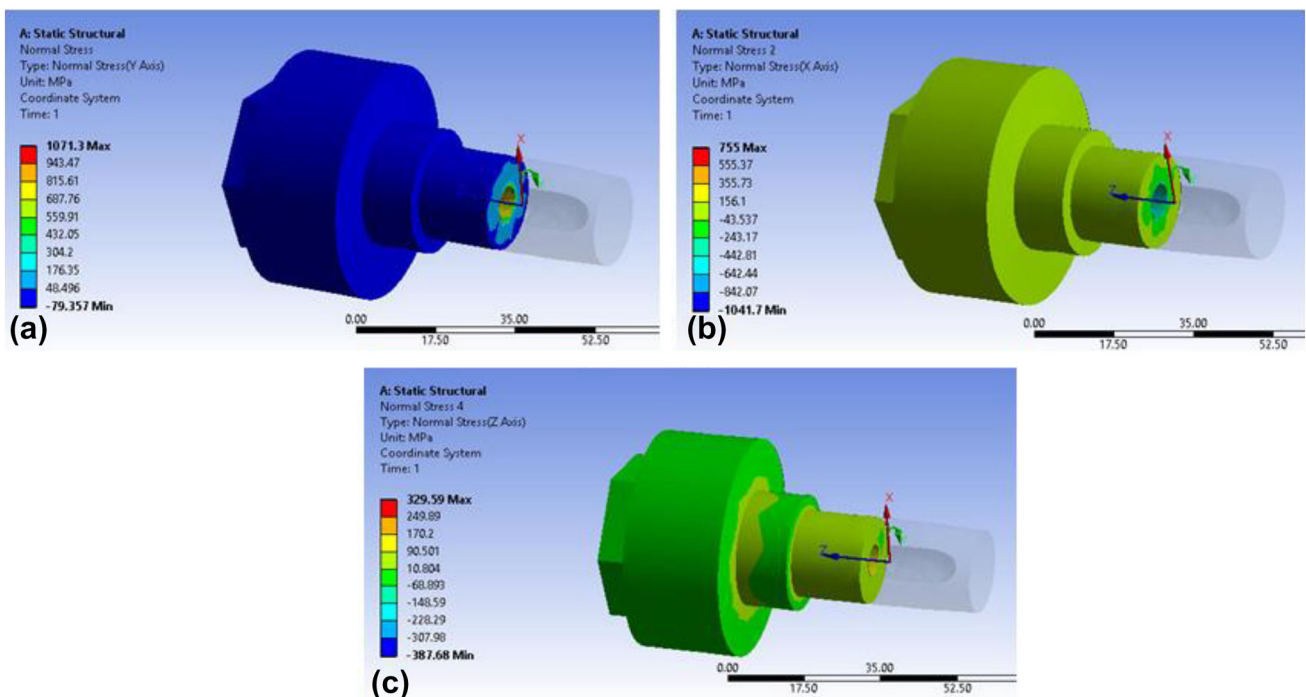


**Fig. 7** a Hoop and b Radial and c Axial stress behaviour under the applied pressure



**Fig. 8** a Fabrication process of the pressure transducer and fabricated models of the transducer

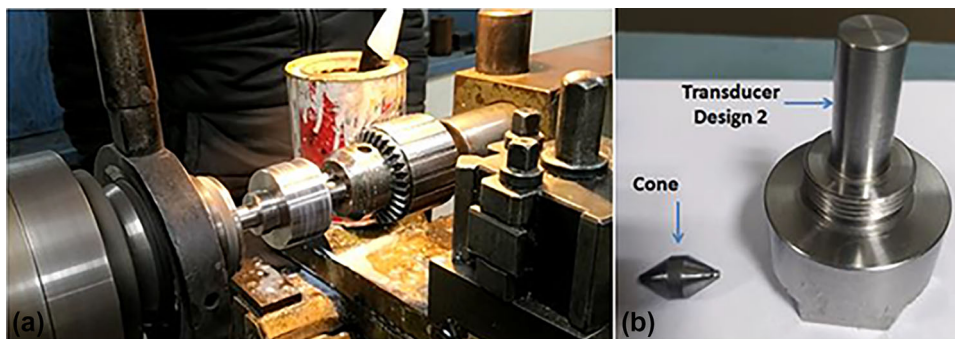
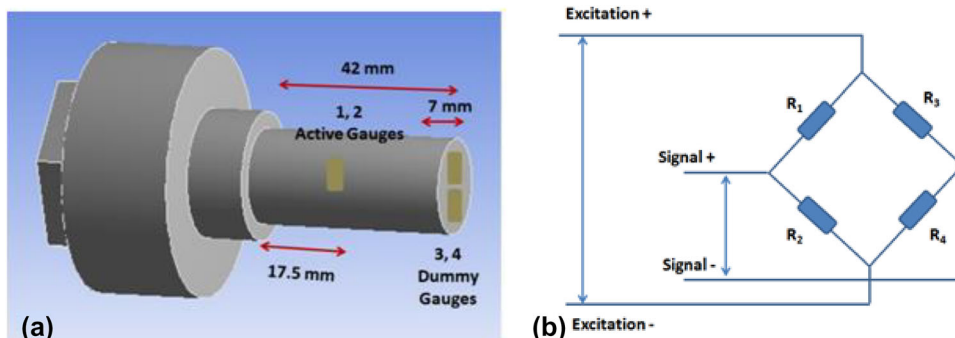


**Fig. 9** A strain gauged pressure transducer with identified locations of strain gauges



$$\frac{V_o}{V_{ex}} = \frac{R_1}{R_1 + R_2} + \frac{R_4}{R_3 + R_4} \tag{4}$$

Because all gauges have the same resistance ( $R = 350$ ) and the gauge factor ( $K$ ) is considered 2 in a balanced condition of the bridge, the production is expected to be zero, and the maximum strain on the hoop direction is denoted by  $\epsilon$ . The Poisson's ratio is denoted by  $\mu$ . However, the change in applied pressure causes the change in resistance. If such changes, then the mathematical model equation for the full Wheatstone bridge is as follows;

$$\frac{V_o}{V_{ex}} = \frac{K\epsilon(1 + \mu)10^{-3}}{2} \tag{5}$$

**5. Result and Discussion**

The calibration of the developed pressure transducer under test is performed by direct comparison with standard pressure generated by the primary national hydraulic pressure standard. During the calibration of the test gauge, the piston of the standard gauge was rotated at approximately 30 rpm through an asynchronous motor. The calibration was done by increasing and decreasing the pressure order. The standard weight combination, the temperature of the piston-cylinder assembly in terms of resistance, the ambient temperature, the humidity, and the instrument's reading of pressure were all observed and recorded. All the calculations of standard generated pressure, regression

analysis, and uncertainty estimation were carried out. Figure 10 shows the complete experimental setup. This setup consists of (i) primary pressure standard (NPL-H1) with the measurement uncertainty of  $\pm 125$  ppm at coverage factor ( $k$ ) of 1, (ii) transducer under test, (iii) 5.5 digital multimeter (DMM) (Hewlett Packard made) of model no. Agilent 34405A (iv) 12 V supply voltage for excitation and (v) di (2-Ethylhexyl) Sebacate oil as a transmitting fluid.

The experiment was conducted at 11 pressure points (0, 100, 200, 300, 400, 500, 600, 700, 800, 900, and 1000 MPa) that were evenly spaced. At each pressure point, six observations were taken, three each in increasing and decreasing sequence of pressure cycles, resulting in 66

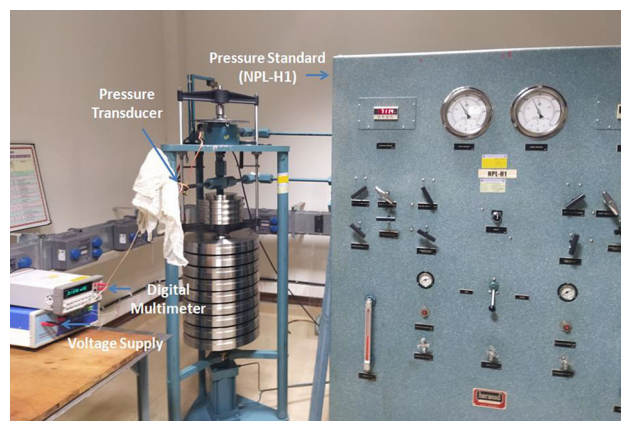


**Fig. 10** Experimental setup of the pressure transducer using National primary standard (NPL-H1)

observations. The findings of these investigations are then utilised to assess the device's performance that has been developed.

### 5.1. Sensitivity in the Transducer

One of the most significant performance characteristics of a transducer is its sensitivity. Equation 5 shows a mathematical model for voltage output with strain. Figure 11 depicts the average change in voltage due to applying pressure. For a pressure range of (0–1000) MPa, an excitation voltage of 12 V results in a 4.30 mV increase in transducer output. It can be seen from the graphs that the transducer's output follows a linear relationship as a function of the input pressure, which is a necessity for any pressure transducer.

### 5.2. Hysteresis in the Transducer

Some intrinsic and unavoidable characteristics, such as anisotropic elasticity of the transducer's material, strain gauge, and adhesive used to affix the strain gauge, produce hysteresis in the transducer. As a result, while the hysteresis error cannot be avoided entirely, it can be minimised. The hysteresis is depicted for the three pressure cycles operating up to the entire range of 1000 MPa (shown in Fig. 12). The transducer can be employed in a rising or decreasing order of pressures for more precise measurements.

The charts also show that all three pressure cycles follow the same course with minor variations in their values. In addition, the maximum hysteresis error is 0.31% of the full-scale pressure.

### 5.3. Measurement Uncertainty Budget

Finally, the estimated measurement uncertainty associated with the pressure transducer is assessed, and the budget is

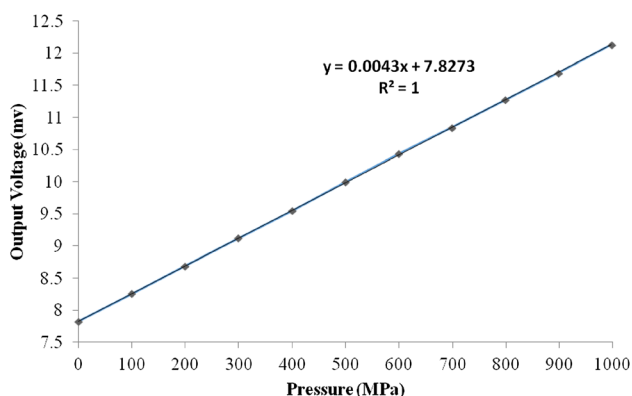


**Fig. 11** Voltage versus pressure curve

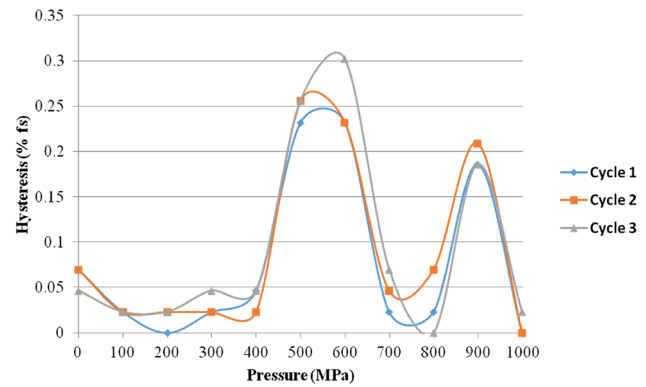


**Fig. 12** Hysteresis error plot

presented in Table 2. Uncertainties due to repeatability ( $u_r$ ), zero setting ( $u_z$ ), hysteresis ( $u_h$ ), resolution ( $u_{res}$ ), and reference standard ( $u_{ref}$ ), are different uncertainty factors taken into account. At a coverage factor of 2, the predicted uncertainty is 0.5% of the full-scale pressure. The detailed methods of uncertainty quantification are described in the following references [37–39]

## 6. Conclusion and Way Forward

Regarding feasibility, precision, accessibility, manufacturability, and economic considerations, pressure measurement employing an essential form strain gauge-type pressure transducer is a strategic and advantageous technology. Taking into account the above, a study of a diaphragm mechanism-based pressure transducer is reported here. Objectives of the reported investigations have varied from developing high-pressure transducers to identifying suitable locations for applying strain gauges or deflection measurements through different means, as mentioned earlier. The sensing element's cylindrical shape was used, providing a cost-effective and straightforward approach for designing a pressure transducer over a wide pressure range. It also ensures a leak-proof and secure connection to the external environment, with no over-constrained contacts. The strain gauge-based pressure transducer is designed, developed, and checked for performance in the pressure range of (0–1000) MPa. The transducer response under pressure is highly linear during the calibration process—the reasonably small hysteresis (maximum 0.31% of full-scale pressure). As a result, the transducer performs satisfactorily within the reasonable measurement uncertainty of 0.5% of the full scale.

The imported high-pressure calibrators and transducers are very expensive. For a highly accurate ultra-high-pressure transducer, the cost is in lakhs of Indian rupees, and it is much higher in the case of a pressure calibrator. Also,

**Table 2** Uncertainty budget of pressure transducer

| Quantity  | Estimate  | Uncertainty | Probability distribution | Type   | Value | Degrees of freedom | Uncertainty contribution     |
|---|-----------|-------------|--------------------------|--------|-------|--------------------|------------------------------|
| ( $X_i$ )   | ( $x_i$ ) | $u(x_i)$    |                          | A or B |       |                    | $u_i (y)^2 / (\text{MPa}^4)$ |
| Pressure  | 997.52    | 1.25E-01    | Normal                   | Type B | 1.0   | $\infty$           | 1.55E-02                     |
| Zero Setting  | 0.003     | 1.73E-03    | Normal                   | Type B | 231.7 | $\infty$           | 1.61E-01                     |
| Resolution  | 0.001     | 2.89E-04    | Normal                   | Type B | 231.7 | $\infty$           | 4.47E-03                     |
| Repeatability   | 0.003     | 0.003       | Rectangular              | Type A | 231.7 | $\infty$           | 5.16E-01                     |
| Hysteresis  | 0.012     | 6.93E-03    | Rectangular              | Type B | 231.7 | $\infty$           | 2.58E + 00                   |
| Regression  | 1.72      | 1.72        | Rectangular              | Type A | 1.0   | $\infty$           | 2.96E + 00                   |
| Combined uncertainty  |           |             |                          |        |       |                    | 2.50                         |
| Relative standard measurement uncertainty at $k = 1$  |           |             |                          |        |       |                    | 2.50E-03                     |
| Estimated effective degrees of freedom  |           |             |                          |        |       |                    | $\infty$                     |
| The estimated value of coverage factor ( $k$ ) at Degrees of Freedom = $\infty$ and 95.45% confidence level |           |             |                          |        |       |                    | 2                            |
| Expanded measurement uncertainty at $k = 2$   |           |             |                          |        |       |                    | 50.05E-04                    |
| Part per million (PPM)  |           |             |                          |        |       |                    | 5005.3                       |
| % age   |           |             |                          |        |       |                    | 0.50                         |

suppose the imported high-pressure calibrator or transducers fails during the testing and calibration. In that case, it remains useless as it cannot be repaired, and a new one must be imported to complete the work. So, every time it is not feasible and economical to import a new one and also to import the new product takes much time. It is expected that from the outcomes of the proposed studies, Indian manufacturers would handle the challenges amicably. This would help them to manufacture accurate and low-cost high-pressure transducers for pressure metrology applications indigenously.

Further, as per quality consciousness, NABL-accredited pressure calibration laboratories are coming to market daily. Many such laboratories require high-pressure measurement systems. Therefore, there is a readymade demand for commercialising such indigenous, low-cost, easy-to-operate high-pressure transducers. This study may also encourage other academia to work in this open-line area of research.

**Acknowledgements** The authors are grateful to Director, CSIR-NPL, for his time-to-time encouragement and motivation. The authors also thank colleagues Mr. Raman Kumar Sharma, Mr. Lalit Kumar, and Dr. Jasveer Singh for their constant support.

## References

- [1] S. Rab, S. Yadav and A. Haleem, A laconic capitulation of high pressure metrology. *Measurement*, 187 (2022) 110226.
- [2] D. K. Aswal (Ed.). *Metrology for inclusive growth of India*. Springer Nature (2020)
- [3] S. Rab, S. Yadav, N. Garg, S. Rajput and D.K. Aswal, Evolution of measurement system and SI units in India. *MAPAN-J. Metrol. Soc India*, 35(4) (2020) 475–490.
- [4] G.I.O.R.G.I.O. Buonanno, G.I.O.R.G.I.O. Ficco, G.A.S.P.A.R.E. Giovinco and G. Molinar, Ten years of experience in modelling pressure balances in liquid media up to few GPa. *Università degli Studi di Cassino, Cassino* (2007).
- [5] S. Yadav, A. Zafer, A. Kumar, N.D. Sharma and D.K. Aswal, Role of national pressure and vacuum metrology in Indian industrial growth and their global metrological equivalence. *MAPAN-J. Metrol. Soc India*, 33(4) (2018) 347–359.
- [6] S. Rab and S. Yadav, Concept of unbroken chain of traceability. *Resonance*, 27(5) (2022) 835–838.
- [7] W. H. Ko, Principles of pressure transducers. *Indwelling and Implantable Pressure Transducers*, (2018) pp.121–132.
- [8] G.F. Molinar, An old instrument in the new technological scenery: the piston gauge in liquid media up to 1 GPa. *Metrologia*, 30(6) (1994) 615.
- [9] R. S. Dadson, S. L. Lewis, and G. N. Peggs, *The pressure balance: theory and practice*. HMSO. (1982)
- [10] N. Dilawar, D. Varandani, A.K. Bandyopadhyay and A.C. Gupta, Characterization of a pneumatic differential pressure transfer standard. *Metrologia*, 40(2) (2003) 74.
- [11] S. Rab, S. Yadav, R.K. Sharma, L. Kumar, V.K. Gupta, A. Zafer and A. Haleem, Development of hydraulic cross floating valve. *Rev. Sci. Instrum.*, 90(8) (2019) 085102.
- [12] A. Kumar, V.N. Thakur, A. Zafer, N.D. Sharma, S. Yadav and D.K. Aswal, Contributions of national standards on the growth of barometric pressure and vacuum industries. *MAPAN-J. Metrol. Soc India*, 34(1) (2019) 13–17.
- [13] J. Singh, L.A. Kumaraswamidhas, N. Bura, S. Rab and N.D. Sharma, Characterization of a standard pneumatic piston gauge using finite element simulation technique vs cross-float, theoretical and Monte Carlo approaches. *Adv. Eng. Softw.*, 150 (2020) 102920.
- [14] S. Rab, A. Zafer, R. Kumar Sharma, L. Kumar, A. Haleem and S. Yadav, National and global status of the high pressure measurement and calibration facilities. *Indian J. Pure Appl. Phys. (IJPAP)*, 60(1) (2022) 38–48.
- [15] S. Yadav, R. Agarwal, D.R. Sharma, A.K. Bandyopadhyay and A.C. Gupta, Modern instrumentation techniques in pressure metrology under static conditions. *MAPAN-J. Metrol. Soc India*, 18(2) (2003) 57–82.



- [16] S. Rab, S. Yadav, A. Haleem, A. Zafer, R. Sharma and L. Kumar, Design and simulation studies on the development of a high pressure cell upto 1.0 GPa for industrial and scientific metrological application. *Mater. Today: Proc.*, 21 (2020) 1632–1636.
- [17] A. Zafer and S. Yadav, Design and development of strain gauge pressure transducer working in high pressure range of 500 MPa using autofrettage and finite element method. *Int. J. Precis Eng. Manuf.*, 19(6) (2018) 793–800.
- [18] G. Molinar, R. Maghenzani and R. Wiśniewski, Free-cylinder, strain-gauge, pressure transducers up to 2 GPa. *Phys B: Condens. Matter*, 265(1–4) (1999) 239–245.
- [19] V.A. Gridchin, V.M. Lubimskyi and M.P. Sarina, Polysilicon strain-gauge transducers. *Sens. Actuators A: Phys.*, 30(3) (1992) 219–223.
- [20] A. Kumar, S. Yadav and R. Agarwal, Design and development of a pressure transducer for high hydrostatic pressure measurements up to 200 MPa. *J. Inst. Eng. (India): Ser. C*, 98(4) (2017) 413–420.
- [21] Timoshenko, S. P., & Goodier, J. N. (1970). *Theory of Elasticity*, 3rd Int. Ed. McGraw-Hill Book Company. Chap. 12.
- [22] J.L.M. Morrison, B. Crossland and J.S.C. Parry, Strength of thick cylinders subjected to repeated internal pressure. *Proc. Inst. Mech. Eng.*, 174(1) (1960) 95–117.
- [23] S. S. Bhavikatti, *Finite element analysis*. New Age International. (2005)
- [24] R. Kumar, S. Rab, B.D. Pant and S. Maji, Design, development and characterization of MEMS silicon diaphragm force sensor. *Vacuum*, 153 (2018) 211–216.
- [25] R. Kumar, S. Rab, B.D. Pant, S. Maji and R.S. Mishra, FEA-based design studies for development of diaphragm force transducers. *MAPAN-J. Metrol. Soc India*, 34(2) (2019) 179–187.
- [26] W. Sabuga, T. Rabault, C. Wüthrich, D. Pražák, M. Chytil, L. Brouwer and A.D. Ahmed, High pressure metrology for industrial applications. *Metrologia*, 54(6) (2017) S108.
- [27] W. Sabuga, D. Pražák and T. Rabault, Recent progress in high pressure metrology in Europe. *EPJ Web Conf.*, 77 (2014) 00006.
- [28] S. Rab, S. Yadav, A. Haleem, A. Zafer, R. Sharma and L. Kumar, Simulation based design analysis of pressure chamber for metrological applications up to 200 MPa. *Indian J. Pure Appl. Phys. (IJPAP)*, 59(3) (2021) 202–205.
- [29] S. Rab, M.A. Sanjid, A. Zafer, A. Haleem and S. Yadav, A new method of optimizing the thickness of metrological surface plate using simulation analysis. *Proc. Inst. Mech. Eng., Part B: J. Eng. Manuf.* (2022). <https://doi.org/10.1177/09544054221116702>.
- [30] K.G. Swift and J.D. Booker, *Manufacturing process selection handbook*. Butterworth-Heinemann (2013).
- [31] S. Kalpakjian, *Manufacturing processes for engineering materials*. Pearson Education India. (1984)
- [32] S. Yadav, O. Prakash, V.K. Gupta and A.K. Bandyopadhyay, The effect of pressure-transmitting fluids in the characterization of a controlled clearance piston gauge up to 1 GPa. *Metrologia*, 44(3) (2007) 222.
- [33] S. Dogra, S. Yadav and A.K. Bandyopadhyay, Computer simulation of 1.0 GPa piston–cylinder assembly using finite element analysis (FEA). *Measurement*, 43(10) (2010) 1345–1354.
- [34] A.Z. Chanchal, R. Singh, A. Kumar and S. Yadav, Review and metrological evolution of primary pressure standard. *Recent Adv. Metrol.: Select Proc. AdMet*, 2021(906) (2022) 363.
- [35] W. Boyes, (Ed.). *Instrumentation reference book*. Butterworth-Heinemann. (2009)
- [36] P.B. Walker, Resistance wire strain gauges. *Aeronaut. J.*, 54(471) (1950) 215–216.
- [37] S. Rab, S. Yadav, A. Zafer, P. Abid Haleem, J.S. Dubey, R. Kumar, R. Sharma and L. Kumar, Comparison of Monte Carlo simulation, least square fitting and calibration factor methods for the evaluation of measurement uncertainty using direct pressure indicating devices. *Mapan -J. Metrol. Soc India*, 34(3) (2019) 305–315.
- [38] S. Yadav, Characterization of dead weight testers and computation of associated uncertainties: a case study of contemporary techniques. *Metrol. Measure.Syst.*, 14(3) (2007) 453–469.
- [39] S. Yadav, V.K. Gupta, O. Prakash and A.K. Bandyopadhyay, Evaluation of associated uncertainties in calibration of direct pressure indicating electromechanical devices. *Measure. Sci. Rev.*, 5(3) (2005) 104–114.

**Publisher's Note** Springer Nature remains neutral with regard to jurisdictional claims in published maps and institutional affiliations.

Springer Nature or its licensor (e.g. a society or other partner) holds exclusive rights to this article under a publishing agreement with the author(s) or other rightsholder(s); author self-archiving of the accepted manuscript version of this article is solely governed by the terms of such publishing agreement and applicable law.